

Mn I hyperfine structure in the near-infrared

Jorge Meléndez ^{*}

Universidade de São Paulo, Cx.P. 3386, São Paulo - SP, 01060-970, Brazil

Accepted ... Received ...

ABSTRACT

Hyperfine interaction constants and hyperfine components of Mn I lines in the near-infrared J and H bands were obtained by fitting the solar spectrum. I identified the 17744-Å solar absorption line as resulting from Mn I, and I discarded the identifications of the 13281.65-Å and 16929.85-Å solar features as a result of Fe I and Mn I, respectively.

Key words: line: identification - line: profiles - Sun: infrared.

1 INTRODUCTION

Mn I shows a large hyperfine structure (HFS) owing to the interaction of the electronic (J) and nuclear (I) angular momenta. The complex profiles have been studied mainly in the ultraviolet and optical regions but not extensively in the infrared region. In the J (1.00 - 1.34 μm) and H (1.49 - 1.80 μm) bands of the solar spectrum there are several Mn I lines (Livingston & Wallace 1991) which show clearly wide hyperfine profiles.

Abt (1952) showed that the profiles and strengths of Mn I stellar absorption lines depend on the HFS. Booth & Blackwell (1983) found that even for weak lines errors of 0.1 dex are possible when HFS is neglected. Hence, it is very important to consider HFS for accurate abundance analysis. The most extensive laboratory work to measure HFS of Mn I lines was carried out by Booth, Shallis & Wells (1983), but unfortunately their measurements only cover ultraviolet and optical lines.

I intend to carry out near-infrared (1-2 μm) spectroscopic observations of metal-rich stars in the Galactic bulge. The infrared region offers the best option to study these very reddened stars because of the high extinction in the optical region. Owing to the lack of HFS data for the Mn I infrared lines, I decided to obtain the HFS components in order to carry out accurate spectroscopic work in the J and H bands.

In Section 2 the hyperfine components are derived, in Section 3 the spectrum synthesis calculations are described and finally the summary of the results is presented in Section 4.

2 HYPERFINE COMPONENTS

The energy hyperfine splittings (ΔE_F) were obtained from the magnetic dipole (A) and electric quadrupole (B) interaction constants (e.g. Emery 1996):

$$\Delta E_F = \frac{1}{2}AC + B \frac{\frac{3}{4}C(C+1) - I(I+1)J(J+1)}{2I(2I-1)J(2J-1)}, \quad (1)$$

where $C = F(F+1) - J(J+1) - I(I+1)$ and $F = J+I, J+I-1, \dots, |J-I|$. For Mn the nuclear spin is $I = 5/2$.

The interaction constants were taken from White & Ritschl (1930), Handrich, Streudel & Walther (1969), Luc & Gerstenkorn (1972), Beynon (1977), Dembczynski et al. (1979), Kronfeldt et al. (1985), Brodzinski et al. (1987), the unpublished results of Guthröhrlein (as given in Brodzinski et al. 1987), and the theoretical values calculated by Per Jönsson (private communication). Jönsson's values are shown in column 3 of Table 11, they were kindly calculated by him using the GRASP relativistic code (Jönsson, Parpia & Froese Fischer 1996).

From the splittings levels (ΔE_F) I computed the wavenumbers of the components using the selection rules $\Delta F = -1, 0, +1$. The air wavelengths were obtained from the wavenumbers using the dispersion formula of Edlén (1966). The relative intensities of the components, $S_{FF'}$, were calculated using the formula (e.g. Emery 1996)

$$S_{FF'} = (2F+1)(2F'+1) \left\{ \begin{matrix} F & F' & 1 \\ J' & J & I \end{matrix} \right\}^2, \quad (2)$$

the quantity in the braces $\{ \}$ is a $6j$ symbol. The $6j$ symbol was calculated using a subroutine taken from Robert Cowan's atomic structure code.

Initially, the relative wavelength positions of the components were calculated with the interaction constants from the given references, and then the interaction constants were adjusted to achieve the best match with the solar spectrum, as described in detail in Section 3. The final values of the

* Affiliated to Seminario Permanente de Astronomia y Ciencias Espaciales, Universidad Nacional Mayor de San Marcos, Perú. E-mail: jorge@iagusp.usp.br

relative positions and intensities of the components, with respect to the main (strongest) hyperfine component, are given in Tables 2-10 and displayed with vertical lines in Figs 1-3.

3 SPECTRUM SYNTHESIS

The code for spectrum synthesis was described by Barbuy (1981, 1982). The synthetic spectrum was calculated with the local thermodynamic equilibrium (LTE) approximation, in successive steps of 0.02 Å in wavelength and convolved with an instrumental profile. A solar model, interpolated in the unpublished grids of model atmospheres by B. Gustafsson, was adopted. The convective fluxes of Gustafsson's models were evaluated using the variant of the mixing-length theory given by Henyey, Vardya & Bodenheimer (1965). Details of the model atmospheres are given by Gustafsson et al. (1975). The adopted solar abundances were those reported by Grevesse, Noels & Sauval (1996), $A_{Mn} = 5.39 \pm 0.03$ dex.

It is important to consider collisional broadening by hydrogen atoms in the Mn I lines because it could affect the determination of hyperfine constants from the solar spectrum. The van der Waals line broadening is given by $\gamma_6/N_H = 17v^{3/5}C_6^{2/5}$ (Allen 1955) where v is velocity, N_H is the number density of hydrogen and C_6 is the interaction constant for collision broadening. C_6 was computed by using the tables of accurate line broadening cross-sections σ of Anstee & O'Mara (1995), Barklem & O'Mara (1997) and Barklem, O'Mara & Ross (1998), for transitions between states s-p/p-s, p-d/d-p, and d-f/f-d, respectively. These tables give σ in terms of the effective principal quantum numbers (n^*) of the upper and lower states of the transition. The obtained C_6 values for the Mn I lines are given in Table 1 among other atomic data.

Atomic (mainly Fe) and CN lines, blended with the Mn I lines, were also included in the calculations. Details about the molecular and atomic infrared line lists are given in Meléndez & Barbuy (1999).

The solar identifications of the Mn I lines were taken from Livingston & Wallace (1991), unless it was established to the contrary. The solar spectrum considered for the comparison with the synthetic spectrum was that given by Livingston & Wallace (1991).

3.1 The 12899-, 13293-, 13319- and 17744-Å lines

These lines were well reproduced with the laboratory interaction constants given in the literature, and I only needed adjust the oscillator strength empirically until the synthetic spectrum matched the solar spectrum. However, it was necessary to correct wavelength positions using the solar spectrum, not only for these lines, but also for all the lines in this paper. Taklif (1990) found differences between measured and predicted wavenumbers of fine structure components. He suggested further work on checking the accuracy of some energy levels.

In Fig. 1 the fittings are shown and in Table 1 the obtained solar wavelengths and $\log(gf)$ values for the main hyperfine components are given. The wavelength positions and oscillator strengths of the others HFS components could be obtained using the relative positions and intensities given

in Tables 2-10. From the fittings, I estimated that the errors for the gf values, given in Table 1, are less than 0.05 dex (without including the error in the assumed abundance).

The 12899- and 13319-Å lines have central depths ($d = 1 - I_{line}/I_{cont}$) of about 0.5 and are affected by NLTE effects, for this reason the observed profile is slightly deeper than the synthetic one.

The 17744-Å line was identified by myself using the laboratory line list of Taklif (1990). This line shows the widest separation between hyperfine components (2 Å). Some part of the solar spectrum that is affected by telluric absorption was not recovered, but the fitting was satisfactory.

3.2 The 12976- and 13281-Å lines

In the case of the 12976- and 13281-Å lines (Fig. 2), I needed to make a correction to the experimental A hyperfine interaction constants in order to reproduce the solar line profiles. The upper levels laboratory A values are highly accurate and therefore were maintained fixed while the lower levels A values were adjusted until the synthetic spectrum matched the solar spectrum.

The most work was required to fit the the 13281-Å line (Fig. 2). In the atlas of Livingston & Wallace (1991) this Mn I line is shown to be blended with a strong Fe I line at 13281.65 Å. This Fe I line was not included in the recent Fe I multiplet table of Nave et al. (1994) and therefore I did not have available the excitation potential for this line. In a first attempt, I assigned a value of 5.5 eV and the line was well reproduced with $\log(gf) = -0.99$. However, I could not fit simultaneously the empirical Fe I and the Mn I lines. So, I thought that the Fe I line would not be the main contributor to the 13281.65-Å solar feature, and I discarded it and tried to fit all the profile as being due only to the Mn I HFS. Then after some adjustment to the A value of the lower level, I obtained the profile shown in Fig. 2 (lower panel).

Livingston & Wallace (1991) used the solar identifications given by Biémont et al. (1985) to assign the 13281.65-Å solar feature to Fe I, but the laboratory intensity of that line is weak (Biémont et al. 1985) and hardly it would be the main contributor to that solar absorption line. I suggest that the 13281.65-Å solar feature is mainly a result of Mn I, specifically to the $F = 5$ to $F' = 4$ hyperfine component.

In Table 11 the solar A values obtained in this work are compared with the experimental values of White & Ritschl (1930) and Beynon (1977). Despite the fact I used incompletely resolved line patterns, the solar values are reliable because they were obtained using accurate level splittings for the upper levels given by Kronfeldt et al. (1985). The solar A values agree better with the earlier determination of White & Ritschl (1930) than with the suggested values given by Beynon (1977). The estimated uncertainties of the solar A values, as deduced from the solar fits, are given between parenthesis in Table 11. B interaction constants could not be obtained from the solar fits, but their contribution to the splitting is usually negligible.

3.3 The 15159-, 15217- and 15262-Å lines

Even though A interaction constants of the lower levels of these lines are well known, there are no laboratory measurements of the A values for the upper levels. In a first attempt

to reproduce the solar profiles, the theoretical A values of Jönsson (Table 11) were employed. The theoretical factors were slightly varied until the best match between synthetic and solar profiles was obtained. In Table 11 the solar A values are compared with the theoretical ones.

In Fig. 3 the fittings are displayed. The blends at 15159.7 and 15216.9 Å are due to Fe I.

3.4 Other Mn I lines probably present in the Sun

Other Mn I infrared lines which are probably present in the Sun are described here.

The 11613-Å line ($e^6S_{5/2} - v^6P_{7/2}$) was identified in the Sun by Swensson et al. (1973). This very weak line is affected by telluric absorption and it was not possible to perform a reliable fitting. I found $\log(gf) \lesssim -0.40$ dex for the main hyperfine component of this line.

In the list of the solar spectrum lines by Ramsauer, Solanki & Biémont (1995) the 16929.85-Å line ($e^4P_{3/2} - 9p^8P_{5/2}$) was identified as owing to Mn I. Despite the fact that the theoretical oscillator strength given by Kurucz (1995) is very small [$\log(gf) = -3.2$] and the excitation potential relatively high (6.4 eV), I tried to fit this line. It was necessary to increase by about four orders of magnitude the theoretical oscillator strength in order to fit the solar line depth. I also noted that it was impossible to fit the overall profile of that line using the theoretical interaction constants of Jönsson ($A = -0.001 \text{ cm}^{-1}$ and $B = 0.003 \text{ cm}^{-1}$ for the $e^4P_{3/2}$ state, and $A = 0.025 \text{ cm}^{-1}$ for $9p^8P_{5/2}$). Even with reasonable variations in the A values, it was not possible to fit the profile. So, I suggest that the identification of that feature, given by Ramsauer et al. (1995), could be wrong.

Using the laboratory line list of Taklif (1990) I identified the 15967 ($e^8D_{11/2} - z^8F_{13/2}$), 16707 ($e^6S_{5/2} - w^6P_{7/2}$), 17325 ($e^6D_{9/2} - w^6F_{11/2}$), 17339 ($e^6D_{7/2} - w^6F_{9/2}$) and 17349 ($e^6D_{5/2} - w^6F_{7/2}$) Å lines in the solar spectrum, but they are severely blended, most of them with unknown contributors, therefore it was not possible to perform reliable fittings for these lines.

4 SUMMARY

Applying spectrum synthesis calculations I reproduced successfully the hyperfine pattern of the Mn I near infrared lines present in the J and H bands of the solar spectrum. Using the solar spectrum, new values for five hyperfine interaction constants were obtained.

According to the results given in this work the principal contributor to the 13281.65-Å solar feature is the main hyperfine component $F = 5$ to $F' = 4$ and not Fe I. On the other hand, I discard the identification of the 16929.85-Å solar line as resulting from Mn I.

The relative positions and intensities of the hyperfine components were given, and also the oscillator strength and wavelength of the principal component. So, I have obtained all the information that I need about Mn I before starting to analyse accurately the spectrum of other cool stars in the near infrared region. However, laboratory measurements are necessary to improve the accuracy of the energy levels and to determine more accurate HFS splittings.

ACKNOWLEDGEMENTS

The calculations were carried out on a DEC Alpha 300/700 workstation provided by FAPESP. The author thanks support by FAPESP fellowship 97/0109-8. He is also grateful to Per Jönsson for the calculation of the theoretical hyperfine interaction constants. NSO/Kitt Peak FTS data used here were produced by NSF/NOAO.

REFERENCES

- Abt A. 1952, ApJ, 115, 199
 Allen C. W., 1955, Astrophysical Quantities, The Athlone Press, London
 Anstee S. D., O'Mara B. J., 1995, MNRAS, 276, 859
 Barklem P., O'Mara B. J., 1997, MNRAS, 290, 102
 Barklem P., O'Mara B. J., Ross J. E., 1998, MNRAS 296, 1057
 Barbuy B., 1981, A&A, 101, 365
 Barbuy B., 1982, PhD thesis, Univ. Paris VII
 Beynon T. G. R., 1977, A&A, 61, 853
 Biémont E., Brault J. W., Delbouille L., Roland G., 1985, A&A, 61, 107
 Booth A. J., & Blackwell D. E., 1983, MNRAS, 204, 777
 Booth A. J., Shallis M. J., Wells M., 1983, MNRAS, 205, 191
 Brodzinski T., Kronfeldt H., Kropp J., Winkler R., 1987, Z. Phys. D, 7, 161
 Dembczynski J., Ertmer W., Johann U., Penselin S., Stinner P., 1979, Z. Phys. A., 291, 207
 Edlén B., 1966, Metrologia, 2, 71
 Emery G. T., 1996, Atomic, Molecular & Optical Physics Handbook, ed. Drake, G. W. F., American Institute of Physics, Woodbury, NY
 Gustafsson B., Bell R. A., Eriksson K., Nordlund Å., 1975, A&A, 42, 407
 Grevesse, N., Noels, A., Sauval, J., 1996, in ASP Conf. Ser. 99, eds. S.S. Holt, G. Sonneborn, p. 117
 Handrich E., Streudel A., Walther H., 1969, Phys.Lett., 29A, 486
 Henyey L., Vardya M. S., Bodenheimer P., 1965, ApJ, 142, 841
 Jönsson P., Parpia F. A., Froese Fischer C., 1996, Comput. Phys. Commun. 96, 301
 Kronfeldt H. D., Kropp J. R., Subaric A., Winkler R., 1985, Z. Phys. A., 322, 349
 Kurucz R., 1995, CD-ROM 23, Harvard-Smithsonian Center for Astrophysics
 Livingston W., Wallace L., 1991, An Atlas of the Solar Spectrum in the Infrared (1.1 to 5.4 μm). National Solar Obs., Tech. Rep. 91-001, Tucson, AZ
 Luc P., Gerstenkorn S., 1972, A&A, 18, 209
 Meléndez J., Barbuy B., 1999, submitted to ApJS
 Nave G., Johansson S., Learner R. C. M., Thorne P., Brault J. W., 1994, ApJS, 94, 221
 Ramsauer J., Solanki S. K., Biémont E., 1995, A&AS
 Swensson J. W., Benedict W. S., Delbouille L., Roland G., 1973, Mém. Soc. R. Sci. Liège, vol. 5
 Taklif A. G., 1990, Physica Scripta, 42, 69
 White H. E., Ritschl R., 1930, Phys. Rev., 35, 1146

Table 1. Mn I atomic lines in the *J* and *H* bands

Wavelength ^a (Å)	Transition	χ^b (eV)	$\log(gf)^c$	C_6 (10^{-31} $\text{cm}^6 \text{s}^{-1}$)
12899.87	$a^6D_{9/2} - z^6P_{7/2}$	2.114	-1.76	0.21
12976.05	$a^4D_{7/2} - z^4P_{5/2}$	2.889	-1.57	0.20
13281.63	$a^4D_{5/2} - z^4P_{3/2}$	2.920	-1.80	0.20
13293.82	$a^6D_{7/2} - z^6P_{7/2}$	2.143	-2.27	0.21
13319.06	$a^6D_{7/2} - z^6P_{5/2}$	2.143	-2.00	0.21
15159.21	$e^8S_{7/2} - y^8P_{9/2}$	4.889	-0.12	5.49
15217.76	$e^8S_{7/2} - y^8P_{7/2}$	4.889	-0.19	5.46
15262.50	$e^8S_{7/2} - y^8P_{5/2}$	4.889	-0.28	5.44
17743.58	$y^6P_{7/2} - e^6S_{5/2}$	4.435	-1.37	3.94

^a Wavelength for the main hyperfine component as obtained from the solar spectrum

^b Excitation energy for the lower level (Kurucz 1995)

^c Value determined in this work for the main hyperfine component

Table 2. Hyperfine components (12899 Å)

$\Delta\lambda$ (Å)	relative intensities	$F - F'$
-0.374	0.3	5 - 6
-0.371	0.7	4 - 5
-0.364	0.8	3 - 4
-0.354	0.6	2 - 3
-0.283	7.7	2 - 2
-0.270	11.9	3 - 3
-0.252	13.5	4 - 4
-0.237	25.0	2 - 1
-0.230	12.4	5 - 5
-0.203	8.0	6 - 6
-0.200	34.0	3 - 2
-0.158	45.8	4 - 3
-0.111	60.7	5 - 4
-0.058	78.6	6 - 5
0.000	100.0	7 - 6

Table 3. Hyperfine components (12975 Å)

$\Delta\lambda$ (Å)	relative intensities	$F - F'$
-0.332	10.3	1 - 0
-0.314	19.8	2 - 1
-0.296	11.0	1 - 1
-0.271	33.0	3 - 2
-0.244	16.5	2 - 2
-0.226	1.8	1 - 2
-0.203	50.4	4 - 3
-0.167	19.2	3 - 3
-0.140	2.2	2 - 3
-0.113	72.5	5 - 4
-0.066	18.1	4 - 4
-0.030	1.6	3 - 4
0.000	100.0	6 - 5
0.056	12.1	5 - 5
0.102	0.7	4 - 5

Table 4. Hyperfine components (13281 Å)

$\Delta\lambda$ (Å)	relative intensities	$F - F'$
-0.328	12.7	2 - 1
-0.311	19.1	1 - 1
-0.302	9.1	0 - 1
-0.260	32.7	3 - 2
-0.235	27.3	2 - 2
-0.218	8.2	1 - 2
-0.151	61.4	4 - 3
-0.118	28.6	3 - 3
-0.093	5.5	2 - 3
0.000	100.0	5 - 4
0.042	20.5	4 - 4
0.075	2.3	3 - 4

Table 5. Hyperfine components (13293 Å)

$\Delta\lambda$ (Å)	relative intensities	$F - F'$
-0.164	10.2	5 - 6
-0.147	15.5	4 - 5
-0.130	16.7	3 - 4
-0.111	14.4	2 - 3
-0.091	9.1	1 - 2
-0.042	16.3	1 - 1
-0.036	19.0	2 - 2
-0.029	28.3	3 - 3
-0.020	44.1	4 - 4
-0.011	67.5	5 - 5
0.000	100.0	6 - 6
0.013	9.1	2 - 1
0.045	14.4	3 - 2
0.080	16.7	4 - 3
0.116	15.5	5 - 4
0.154	10.2	6 - 5

Table 6. Hyperfine components (13319 Å)

$\Delta\lambda$ (Å)	relative intensities	$F - F'$
-0.295	0.7	4 - 5
-0.266	1.6	3 - 4
-0.235	2.2	2 - 3
-0.202	1.8	1 - 2
-0.161	12.1	5 - 5
-0.159	18.1	4 - 4
-0.155	19.2	3 - 3
-0.150	16.5	2 - 2
-0.145	11.0	1 - 1
-0.117	10.3	1 - 0
-0.093	19.8	2 - 1
-0.071	33.0	3 - 2
-0.048	50.4	4 - 3
-0.025	72.5	5 - 4
0.000	100.0	6 - 5

Table 7. Hyperfine components (15159 Å)

$\Delta\lambda$ (Å)	relative intensities	$F - F'$
-0.183	34.0	2 - 3
-0.183	25.0	1 - 2
-0.166	45.8	3 - 4
-0.129	60.7	4 - 5
-0.074	78.6	5 - 6
-0.070	7.7	2 - 2
-0.014	11.9	3 - 3
0.000	100.0	6 - 7
0.061	13.5	4 - 4
0.100	0.6	3 - 2
0.154	12.4	5 - 5
0.212	0.8	4 - 3
0.265	8.0	6 - 6
0.343	0.7	5 - 4
0.493	0.3	6 - 5

Table 8. Hyperfine components (15217 Å)

$\Delta\lambda$ (Å)	relative intensities	$F - F'$
-0.349	15.5	4 - 5
-0.345	16.7	3 - 4
-0.342	10.2	5 - 6
-0.331	14.4	2 - 3
-0.306	9.1	1 - 2
-0.213	16.3	1 - 1
-0.192	19.0	2 - 2
-0.160	28.3	3 - 3
-0.117	44.1	4 - 4
-0.099	9.1	2 - 1
-0.064	67.5	5 - 5
-0.021	14.4	3 - 2
0.000	100.0	6 - 6
0.068	16.7	4 - 3
0.168	15.5	5 - 4
0.278	10.2	6 - 5

Table 9. Hyperfine components (15262 Å)

$\Delta\lambda$ (Å)	relative intensities	$F - F'$
-0.630	0.7	4 - 5
-0.539	1.6	3 - 4
-0.455	2.2	2 - 3
-0.378	1.8	1 - 2
-0.344	12.1	5 - 5
-0.310	18.1	4 - 4
-0.283	19.2	3 - 3
-0.263	16.5	2 - 2
-0.249	11.0	1 - 1
-0.185	10.3	1 - 0
-0.135	19.8	2 - 1
-0.091	33.0	3 - 2
-0.054	50.4	4 - 3
-0.024	72.5	5 - 4
0.000	100.0	6 - 5

Table 10. Hyperfine components (17744 Å)

$\Delta\lambda$ (Å)	relative intensities	$F - F'$
0.000	100.0	6 - 5
0.246	12.1	5 - 5
0.450	0.7	4 - 5
0.670	72.5	5 - 4
0.875	18.1	4 - 4
1.039	1.6	3 - 4
1.215	50.4	4 - 3
1.379	19.2	3 - 3
1.501	2.2	2 - 3
1.633	33.0	3 - 2
1.756	16.5	2 - 2
1.838	1.8	1 - 2
1.926	19.8	2 - 1
2.008	11.0	1 - 1
2.093	10.3	1 - 0

Table 11. Comparison of magnetic interaction constants (A)

Level	TW $_{\odot}^a$ (cm $^{-1}$)	J98 b (cm $^{-1}$)	WR30 c (cm $^{-1}$)	B77 d (cm $^{-1}$)
a 4 D $_{7/2}$	-0.0057 (0.0005)		-0.0055	-0.004
a 4 D $_{5/2}$	-0.0046 (0.0005)		-0.0042	-0.003
y 8 P $_{9/2}$	0.0165 (0.0015)	0.015		
y 8 P $_{7/2}$	0.0200 (0.0015)	0.018		
y 8 P $_{5/2}$	0.0275 (0.0015)	0.024		

^a This work, from the solar spectrum^b P. Jönsson, private communication^c White & Ritschl (1930)^d Beynon (1977)

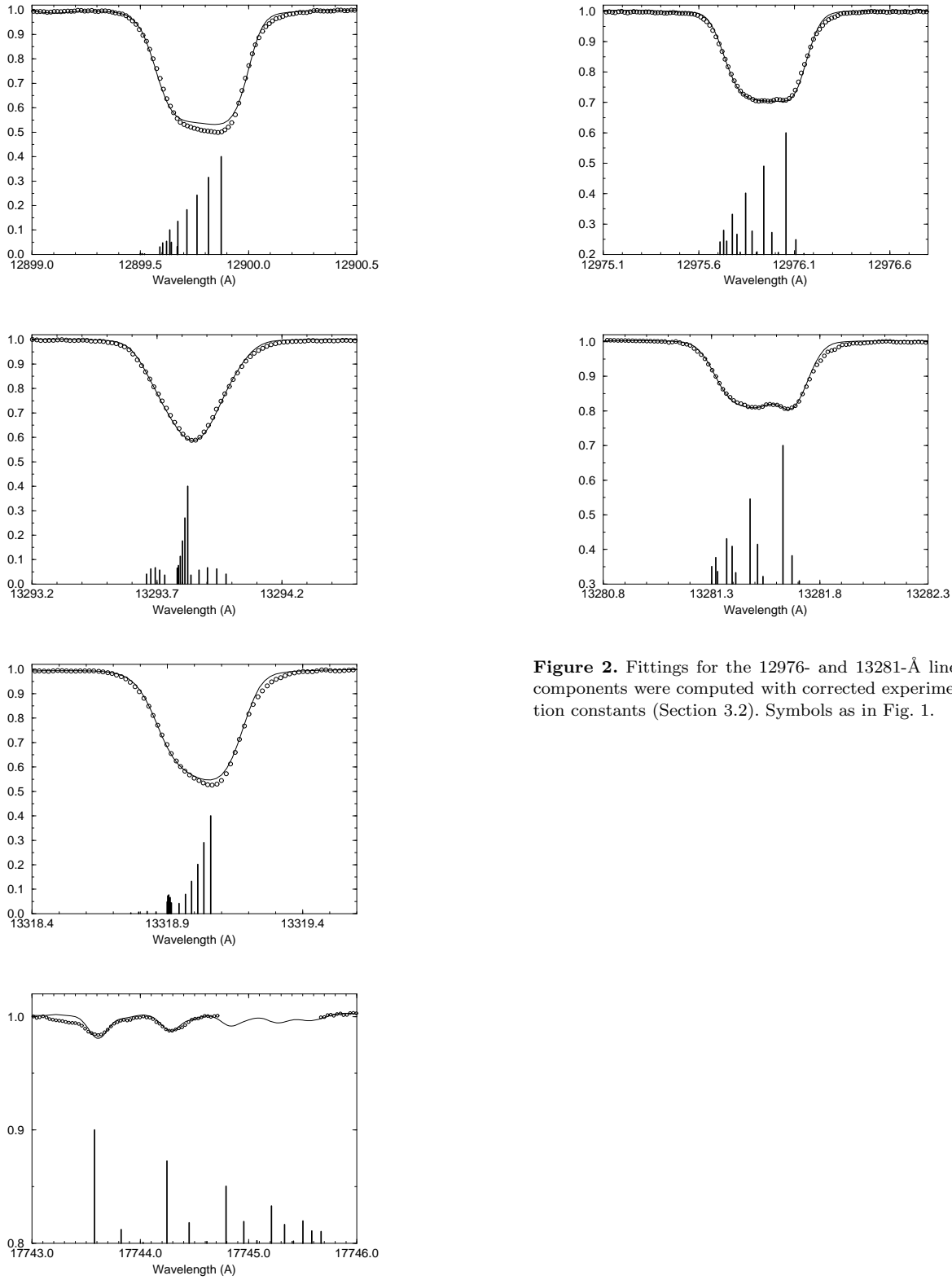


Figure 1. Fittings for the 12899-, 13293-, 13319- and 17744-Å lines. The HFS components were computed without any correction to laboratory interaction constants (Section 3.1). Solar spectrum (circles), synthetic spectrum (solid line) and HFS components (vertical lines).

Figure 2. Fittings for the 12976- and 13281-Å lines. The HFS components were computed with corrected experimental interaction constants (Section 3.2). Symbols as in Fig. 1.

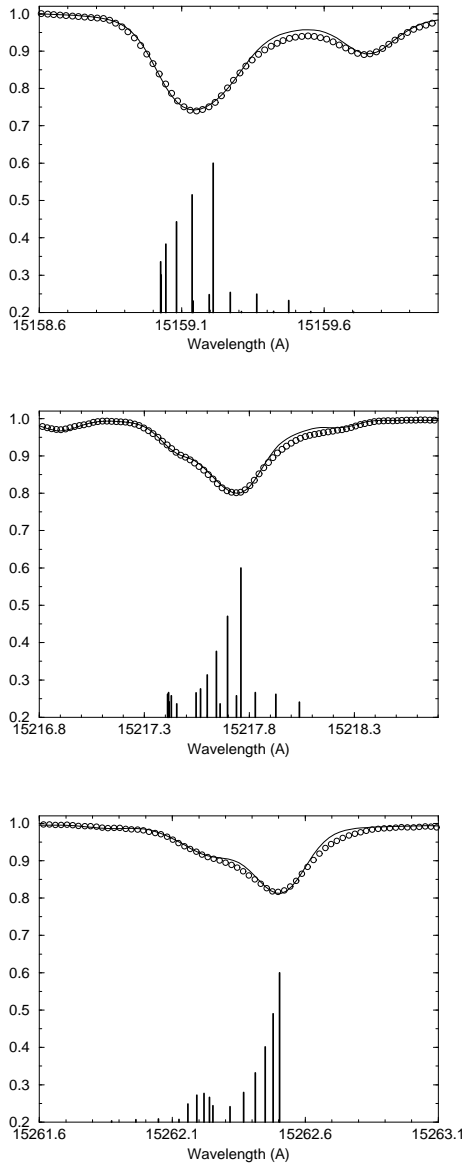


Figure 3. Fittings for the 15159-, 15217- and 15262-Å lines. The HFS components were computed with corrected theoretical interaction constants (Section 3.3). Symbols as in Fig. 1.